

DURATION PARAMETERS FOR THE SELECTION OF GROUND MOTION TIME HISTORIES FOR NON LINEAR ANALYSIS OF EMBANKMENT DAMS

by

Donald E. Yule¹, Enrique E. Matheu², and Michael H. Beaty³

ABSTRACT

Nonlinear dynamic analysis of embankment dams requires a definition of the input motion that goes beyond the specification of a spectral content. The seismic input must be expressed in terms of a time-history realization of the selected design/evaluation earthquake. The problem is complicated by the stress path-dependency of nonlinear constitutive models, and this leads to the commonly accepted practice of using multiple sets of acceleration time histories for these types of analyses. Typically, natural records must be modified to reflect the specified target conditions, and in some cases are complemented with artificially generated time histories to provide a representative set of ground motions. However, the particular characteristics of each time history may lead to appreciable differences in the predicted response. This paper presents a preliminary investigation on the influence of accelerogram characteristics on post-liquefaction deformation analysis of embankment dams. The effects of the earthquake records are evaluated for a simple embankment dam using the two-dimensional finite difference program FLAC and the UBCSAND constitutive model to estimate the dynamic response. Nine earthquake records were selected for evaluation. The sensitivity of the analysis results to the input motion is investigated in terms of the predicted dynamic deformations, as well as the extent and timing of associated liquefaction phenomena.

KEYWORDS: Arias intensity; deformation; duration; earthquake; embankment dam; ground motion; non-linear analysis; seismic.

1.0 INTRODUCTION

Seismic safety evaluations of critical dams for maximum design loads may require advanced analyses to estimate earthquake-induced deformations to assess embankment performance, usually with a performance objective that allows considerable damage but not failure (loss of reservoir). The state-of-the-practices for engineering seismology and geotechnical earthquake engineering currently include nonlinear analyses of embankment dams. A dynamic analysis to assess large embankment deformations using a nonlinear constitutive model results in a technically demanding problem. These analyses are very dependent on the idealization of the real system (e.g., geometry, material properties, constitutive model, and earthquake loading). Facing these challenges requires a strategy to quantify and understand the potential global response of the system.

An important decision in the seismic evaluation process is the selection of the dynamic input. In the case of nonlinear dynamic analysis, the expected earthquake must be expressed as a set of ground motion time histories. For safety evaluations it is important that among the admissible time history realizations, the selected input motions induce an appropriate range of structural responses bounded by a reasonable conservatism in the assignment of seismic hazard parameters. Although this problem may seem intractable because of the number of time-history realizations that could be associated with a given design/evaluation earthquake, realistically there exists a bound for the level of

¹ Research Civil Engineer, Engineer Research and Development Center U.S. Army Corps of Engineers (ERDC), Vicksburg, MS 39180, USA

² Research Structural Engineer, ERDC, Vicksburg, MS, 39810, USA

³ Senior Engineer, Division of Engineering, California Department Water Resources, Sacramento, CA 95814, USA

earthquake response likely to be achieved by the physical system. The quantification of this response requires a good understanding of the dynamic response of the system and the ground motion parameters that characterize the damage potential of the seismic input (USCOLD, 1999). This paper investigates a real world case with liquefaction susceptible soils in the foundation of an embankment dam. All parameters are fixed except the earthquake loading, which is varied with the objective of investigating its effect on the resulting deformation response.

2.0 GROUND MOTION CHARACTERISTICS

Given an acceleration time history, $a_g(t)$, which is assumed representative of the expected earthquake ground motions, different parameters can be employed to characterize its severity and damage potential. An obvious parameter to be considered is the corresponding peak acceleration value (PGA). The use of this descriptor is intuitively natural since accelerations and the resulting inertial forces are directly related by Newton's second law. However, there is not a direct correspondence between PGA and the structural response at the significant natural frequencies of most typical dams. In addition, a large PGA value associated with an isolated spike is not sufficient by itself to generate response conditions leading to significant damage. In spite of these limitations, PGA has remained one of the fundamental parameters used to judge the damage potential of a given acceleration history. An additional peak measure used to characterize a given time acceleration record is given by the corresponding peak ground velocity (PGV). However, amplitude indices such as PGA and PGV offer a limited description of the seismic input and its potential consequences on the structure.

The full frequency content of the earthquake ground motion has a profound influence on the dynamic response of the system. Therefore, a better characterization of a given input motion can be achieved by using some form of spectral representation. In particular, the use of response

spectra (parametric representation of a selected peak response of a family of single-degree-of freedom systems subjected to the particular ground motion) is at the core of earthquake engineering practice. Some scalar descriptors can be defined based on this representation such as the velocity spectrum intensity (SI), which is defined as the integral of the 5%-damping pseudo-velocity spectrum over the period interval (0.1, 2.5) sec (Von Thun et al., 1988). However, these characterizations do not provide a direct description of the duration or the time varying features of a given input motion. In fact, it is possible to generate multiple time history realizations with very different characteristics that correspond to similar response spectra. When nonlinear behavior is taken into account, these time varying features may have a strong influence on the computed response.

One of the simplest measures of the time domain character of a record is the duration of strong motion. Different approaches can be used to describe the duration of the strong motion in an acceleration time history. A common measure is given by the bracketed duration (T_d), defined as the time elapsed between the first and last exceedances of a threshold acceleration value (0.05g). In addition, other descriptors have been proposed to globally quantify the time varying characteristics of a given input motion. For example, the Arias intensity (I_a) provides a measure of the energy delivered by the accelerogram and is defined as follows (Arias, 1970):

$$I_d = \pi / (2 * g) \int (a_t)^2 dt$$

A related duration measure is given by the 5-95% Arias intensity duration (D_{5-95}), defined as the time required for I_a to increase from 5 to 95% of its final value. A further consideration in the time domain character of an earthquake record is the potential for directivity effects. These effects can have a significant influence on the record characteristics, particularly at near field sites, and may produce large velocity pulses for forward directivity conditions (Somerville et al., 1997).

3.0 MODELING NONLINEAR BEHAVIOR (UBCSAND MODEL)

This analytical study assumes a simple embankment section and estimates its dynamic response using the two dimensional FLAC finite difference program (Itasca, 2000) and the nonlinear UBCSAND constitutive model. The FLAC program models the soil structure as a collection of grid zones or elements and solves the coupled stress-hydraulic flow problem using an explicit time stepping approach. The UBCSAND constitutive model is a relatively simple elastoplastic model based on an assumed hyperbolic relation between stress ratio and plastic shear strain. Increments of plastic volumetric change are related to increments of plastic shear strain through a non-associative flow rule. As a plasticity model, it includes such features as a yield surface and definitions for loading, unloading, and hardening. It can be considered a variation of the Mohr- Coulomb plasticity model where friction and dilation angles are varied to incorporate the yield loci and flow rule. UBCSAND captures the characteristic behavior of sand as observed in laboratory tests under monotonic and cyclic loading conditions. Its effective stress formulation represents the behavior of the soil skeleton with the effect of pore fluid introduced through its volumetric stiffness. This allows the model to simulate the drained, undrained, and partiallydrained response that is observed in laboratory tests using the same set of model parameters. Further description of the model can be found in Byrne et al. (2003, 2004).

4.0 CASE STUDY

This section summarizes the model geometry, material properties, the investigated nine earthquake records and the deformation analysis results in this study.

4.1 Model Geometry and Material Properties

The geometric configuration of the numerical model is shown in Figure 1. The adopted

embankment section is 40 m high with a 2.5:1 upstream slope and a 2:1 downstream slope. The shells of the dam were assumed to be sandy with a density represented by an average corrected SPT blowcount, $(N_1)_{60}$, of about 30. The dam has a wide central clayey core and a 10-meterdeep cutoff trench. The dam is founded on 20 m of alluvium over bedrock, and the reservoir is 37 m in depth. A continuous liquefiable foundation layer, between 2.5 m and 10 m in depth, was assumed to have an average $(N_1)_{60}$ of 12. Elastic and plastic parameters selected for the UBCSAND model were typical for the assumed materials. These properties were approximated from published data and model calibrations (Byrne et al., 2004). These calibrations included comparisons of liquefaction predictions to the semi-empirical liquefaction chart adopted by the NCEER workshop (Youd et al., 2001). The hydraulic flow option of FLAC was used to estimate the phreatic surface and initial pore water pressures. This analysis produced full saturation within most of the upstream shell, the clayey core, and the alluvial foundation. Much of the downstream shell was unsaturated. The dynamic analysis was performed in fully coupled mode which considers both the stress-strain response and hydraulic flow. This permitted redistribution of excess pore pressures during shaking as predicted by Darcy's law.

4.2 Earthquake Input Motions

The suite of nine earthquake records used in this investigation can be divided into three distinct groups: three accelerograms originally developed for a dam in CA (F1, F2, and F3), another set of three developed for a dam in the CEUS (W1, W2, and W3), and a third set chosen to investigate the effect of large velocity pulses in near field locations. The first two sets contain accelerograms that have been modified to meet their respective target design spectra. The spectral content of the third set of records was not modified. Pertinent information on these earthquake records are shown in Table 1, and the corresponding time history parameters are shown in Table 2. The acceleration time histories are shown in Figure 2, and their corresponding response spectra and Arias

intensity plots are presented in Figure 3. To simplify the final interpretations, the following two approximations were made regarding the definition of the seismic loading: 1) vertical input motions were not considered, and 2) the scaled surface motions were applied directly to the base of the model without modification to account for depth.

4.3 Deformation Analysis Results

The response of the system, specifically the deformation of the embankment, exhibited similar behavior for the entire suite of earthquake loadings. A significant slide plane initiated near the base of the liquefiable foundation materials beneath the upstream shell. The loss of foundation strength and stiffness due to pore pressure generation caused the upstream shell to deform, shearing the core and producing vertical deformations of the crest. Figure 4 presents results from a typical case with plots of final grid displacements, contours of maximum excess pore pressure, and contours of maximum shear strains. As expected the zones of maximum pore pressure development and shearing coincide. Although this mode of response was common to all of the earthquakes analyzed, the amount of deformation (system performance) and its evolution were dependent on the specifics of the earthquake time history.

The metric used to investigate the embankment response was the maximum grid point displacement relative to grid base (D_{max}). This global response quantity is tabulated in Table 2, which shows D_{max} for each record. The location of maximum displacement in general was near the upstream toe within the shear plane transecting the liquefiable foundation zone. Table 2 shows that PGA is inconclusive as a predictor of embankment deformations. Earthquake cases F1-F3 with the same PGA have significantly different deformations ranging from 1.9 m to 5.9 m, and similar results were found for cases W1-W3 where deformations ranged from 2.7 m to 4.2 m. Since the time histories for these two cases were matched to their respective target design spectra, we also conclude that spectral content is not solely sufficient for quantifying potential

permanent deformations. This result is consistent with the PGA result as a response spectrum represents a set of peak responses of linear elastic oscillators, and it offers a poor analog for non-linear plastic deformation behavior (Beatty, 2001). The fact that the D_{max} predictions do not appear to be well correlated to PGA is also evident in the third suite of records. Based on the results presented in Table 2, similar observations can be made regarding PGV. Considering the inconclusive performance of PGA and PGV as parameters for gauging potential earthquake-induced deformations, other parameters that combine duration and strength of shaking may serve as more consistent predictors of global dynamic responses involving complex phenomena such as cyclic non-linear behavior of soils. Similar arguments can be made for the development of predictors to estimate the sliding response of a concrete dam, which is characterized by complicated frictional behavior. A natural parameter for consideration is the Arias intensity, which has been investigated as damage indicator in the context of earthquake induced landslides, liquefaction potential of soil deposits and building structures. Figure 5 shows the maximum permanent displacement (D_{max}) as a function of Arias intensity (I_a) and bracketed duration (T_d) for the three sets of records. The plots also include different amplitude scaling levels for one record in each of the W and F sets, as well as three amplitude scaling levels for each record in the third set. Several trends are apparent: (1) for the case of multiple levels of the same record, the maximum displacement varies roughly linearly with Arias Intensity, (2) similar type of linear correlation can be observed if records consistent with a given target spectrum are considered (sets F and W), and (3) each case (set of multiple levels of the same record or expanded set including spectrum-matched records) appears to have its own relationship between maximum permanent displacement and Arias intensity. Similar observations can be made regarding the correlation with bracketed duration, although the data points seem more scattered particularly for those cases associated with multiple levels of the same record. This can be explained considering

that the bracketed duration does not vary smoothly as a function of the amplitude scaling level. It contains only information on the end-points defining the duration of strong shaking, without directly quantifying its severity. Excess pore water pressure generation is another critically important phenomenon that was investigated for the spectrum-compatible cases (F and W). For each record, the evolution of excess pore pressure at a critical location (point A, Figure 1) is plotted in Figure 6 as a function of the percentage of the corresponding Arias intensity, which implicitly represents the amount of energy delivered. Of these two sets of results, F1 stands out as a distinctive case where considerable excess pore pressures exist, but a significant fraction of the total energy is yet to be delivered. This case exhibited the largest predicted deformation from all the cases. This confirms the fact that the damage potential of a load case is related to energy delivery characteristics.

5.0 CONCLUSION

This study presents a preliminary investigation of the influence of accelerogram characteristics on deformation predictions for embankment dams on liquefiable foundations. The deformation response was evaluated using the two-dimensional finite difference program FLAC and the UBCSAND constitutive model. Nine earthquake records were selected for this study, and each case analyzed resulted in predictions of widespread foundation liquefaction leading to significant permanent deformations. The results show that PGA and PGV are not sufficient characterizations for gauging the potential of a particular earthquake time history to produce significant permanent deformations. Duration parameters such as the Arias Intensity offer a more adequate representation of the damage potential. For the particular cases investigated, the relationship between Arias Intensity and maximum permanent displacement was approximately linear for each self-similar suite of records. However, comprehensive studies are needed to define the different factors affecting this correlation. Further research into characterizing

the energy delivery is needed to estimate the capacity of an earthquake time history to generate permanent deformations in an embankment dam.

6.0 ACKNOWLEDGMENTS

Preparation of this paper was sponsored and supported by the U.S. Army Corps of Engineers. Permission to publish has been granted by Director, Geotechnical and Structures Laboratory, U.S. Army Engineer Research and Development Center.

7.0 REFERENCES

- Arias, A. (1970). "A Measure of Earthquake Intensity," in *Seismic Design for Nuclear Power Plants*, MIT Press, Cambridge, MA.
- Beatty, M. H. (2001). "A Synthesized Approach for Estimating Liquefaction-Induced Displacements of Geotechnical Structures." Ph.D. Thesis, University of British Columbia, Department of Civil Engineering, Vancouver, Canada.
- Byrne, P. M., Park, S. S., and Beatty, M. (2003). "Seismic Liquefaction: Centrifuge and Numerical Modeling," in *Proc. 3rd International FLAC Symposium*, Balkema.
- Byrne, P. M., Park, S. S., Beatty, M., Sharp, M., Gonzalez, L., and Abdoun, T. (2004). "Numerical Modeling of Liquefaction and Comparison with Centrifuge Tests," *Canadian Geotechnical Journal*, in press.
- Itasca (2000). *FLAC, Version 4.0*. Itasca Consulting Group Inc., Minneapolis.
- Somerville, P. G., Smith, N. F., Graves, R. W., and Abrahamson, N. A. (1997). "Modification of Empirical Strong Ground Motion Attenuation Relations to Include the Amplitude and Duration Effects of Rupture Directivity," *Seismological Research Letters*, Vol. 68, No. 1, pp. 199-222.

USCOLD (1999). Updated Guidelines for Selecting Seismic Parameters for Dam Projects, U.S. Committee on Large Dams, Denver, CO.

Von Thun, J. L., Rochim, L. H., Scott, G. A., and Wilson, J. A. (1988). "Earthquake Ground Motions for Design and Analysis of Dams," in Earthquake Engineering and Soil Dynamics II – Recent Advance in Ground Motion Evaluation, ASCE, New York, NY.

W.D.L., Harder Jr. L.F., Hynes, M.E., Ishihara, K., Koester, J.P., Liao, S.S.C., Marcuson III, W.F., Martin, G.R., Mitchell, J.K., Moriwaki, Y., Power, M.S., Robertson, R.K., Seed, H.B., and Stokoe II, K.H. (2001). "Liquefaction Resistance of Soils: Summary Report from the 1996 NCEER and 1998 NCEER/NSF Workshops on Evaluation of Liquefaction Resistance of Soils," Journal of Geotechnical and Geoenvironmental Engineering, Vol. 127, No. 10, pp. 817-833.

Table 1. Earthquake records used to develop the time histories used in the analyses

Case	Original Earthquake	Station	M	Closest Dist. km	PGA g
W1	Chi-Chi, Taiwan (1999)	Chiayi-Sanhe Sch. / 360 deg	7.6	21.5	0.28
W2	Landers, CA (1992)	Joshua Tree Fire Sta. / 90 deg	7.3	13.7	0.36
W3	Chi-Chi, Taiwan (1999)	Donghe Sch., WGGK / 90 deg	7.6	13.3	0.36
F1	Imperial Valley, CA (1979)	Cerro Prieto /180 deg	6.5	20.0	0.38
F2	Chalfant Valley, CA (1986)	Bishop – Paradise Lodge / 160 deg	6.2	17.0	0.38
F3	San Fernando, CA (1971)	Pasadena – Old Seism. Lab. / 270 deg	6.6	27.8	0.38
D1	Denali, AK (2002)	TAPS Pumping Sta. No. 10 / 51 deg	7.9	3.0	0.34
L1	Landers, CA (1992)	Lucerne Valley / 360 deg	7.3	2.0	0.81
R1	Northridge, CA (1994)	Rinaldi R.S. / 229 deg	7.0	8.6	0.84

Youd, T.L., Idriss, I.M., Andrus, R.D., Arango, I., Castro, G., Christian, J.T., Dobry, R., Finn,

Table 2. Maximum permanent deformations for various cases

Case (Scaling)	PGA g	PGV cm/sec	Sa _(1 sec) g	Ia cm/sec	D ₅₋₉₅ sec	Td sec	D _{max} m
W1 (1.0)	0.28	19.6	0.40	215	33.1	41.7	3.3
W2 (1.0)	0.36	35.6	0.40	202	38.0	40.6	4.2
W3 (1.0)	0.36	26.5	0.40	138	29.2	31.3	2.7
F1 (1.0)	0.38	22.6	0.30	815	39.5	57.0	6.0
F2 (1.0)	0.38	29.2	0.30	356	15.6	35.1	2.3
F3 (1.0)	0.38	35.7	0.30	262	14.1	22.4	1.9
D1 (1.0)	0.34	113.5	1.00	188	19.0	30.9	3.3
L1 (0.5)	0.41	15.8	0.15	977	13.6	29.2	0.9
R1 (0.5)	0.42	86.0	0.81	1067	7.1	14.9	1.8

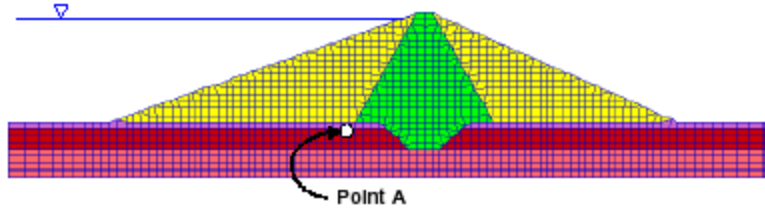


Figure 1. Embankment cross-section showing grid and material zones.

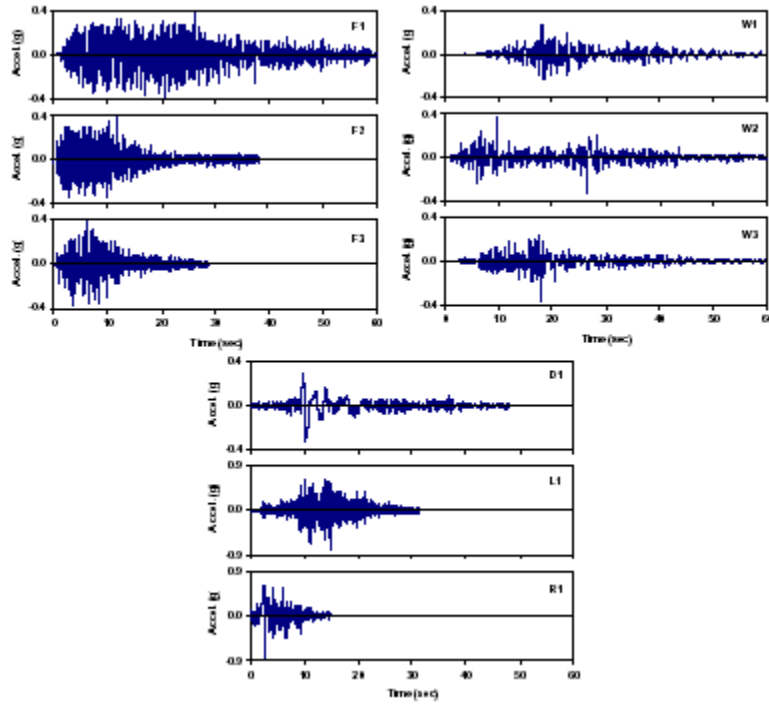


Figure 2. Acceleration time histories for earthquake records used in study.

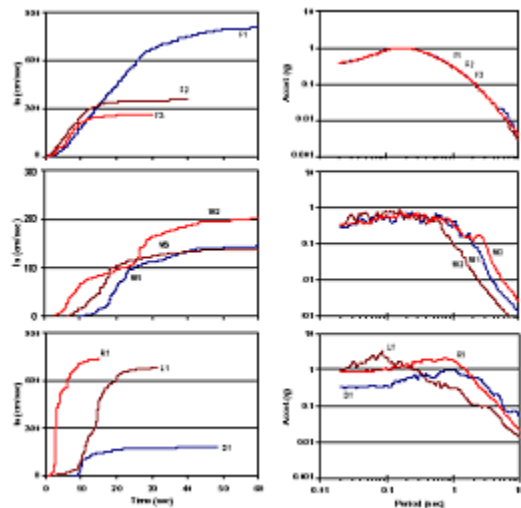


Figure 3. Arias Intensity and response spectra plots for earthquake records used in this study.

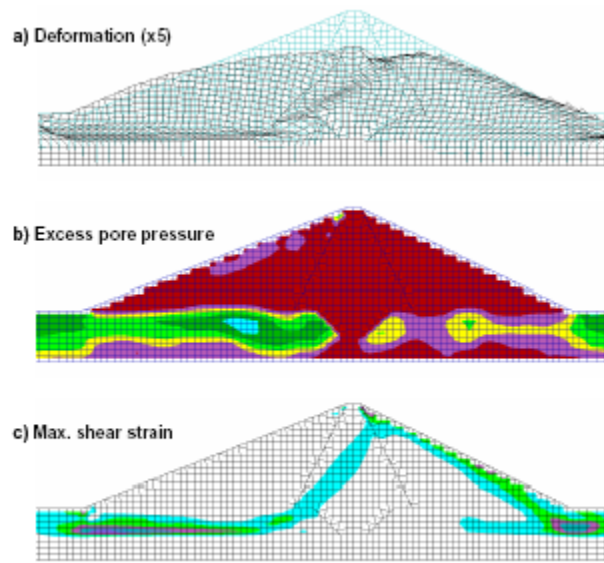


Figure 4. Typical deformation analysis results showing final grid deformation, maximum excess pore pressure, and maximum shear strain.

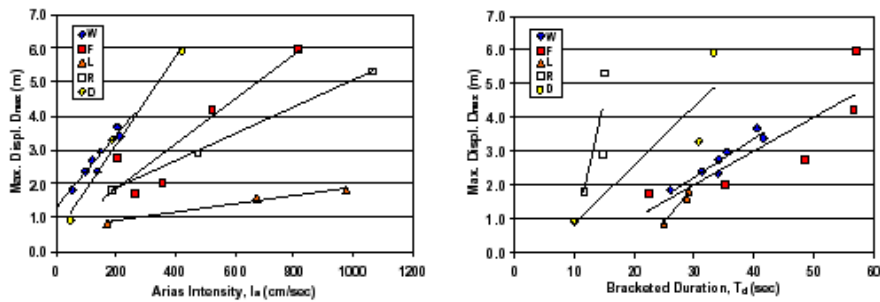


Figure 5. Maximum displacement as a function of total Arias intensity and bracketed duration.

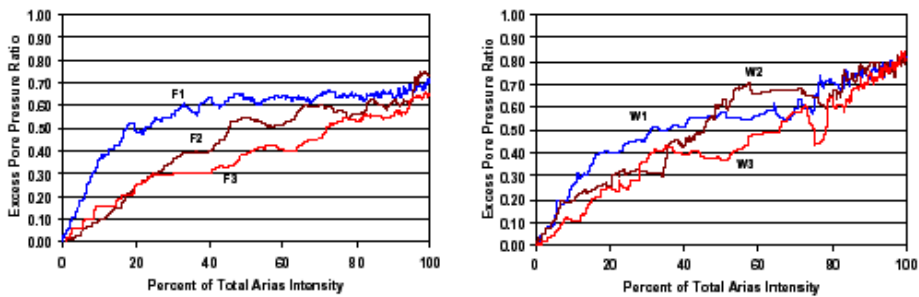


Figure 6. Excess pore pressure ratio in terms of percentage of total Arias intensity.